Vorticity-based modeling of gravity currents penetrating into ambients with arbitrary shear and density stratification

Mohamad M. Nasr-Azadani, Presenting Author and Eckart Meiburg

Department of Mechanical Engineering,
University of California Santa Barbara, Santa Barbara, CA 93106
mmnasr@engineering.ucsb.edu meiburg@engineering.ucsb.edu

Abstract

We develop a vorticity-based approach for modeling quasi-steady, supercritical gravity currents propagating into a finite-height channel with arbitrary density and velocity stratification. The model enforces the conservation of mass, horizontal and vertical momentum. In contrast to previous approaches it does not rely on empirical, energy-based closure assumptions. Instead, the effective energy loss of the flow can be calculated *a posteriori*. The present model results in the formulation of a second order, nonlinear ODE that can be solved in a straightforward fashion to determine the gravity current velocity, along with the downstream ambient velocity and density profiles. Comparisons between model predictions and DNS simulations show excellent agreement.

1 Introduction

Gravity currents are driven by horizontal gradients in the hydrostatic pressure as a result of density differences (Benjamin (1968), Linden (2012)). Depending on the source of these density differences, various types of gravity currents can be distinguished (cf. Moncrieff (1992), Simpson (1997), Meiburg and Kneller (2010)). In the atmosphere, gravity currents frequently interact with background shear and/or density stratification. For instance, severe thunderstorms can produce gravity currents of cold air traveling along the ground whose dynamics are affected by existing shear in the ambient atmosphere (Bryan and Rotunno (2014)), thereby resulting in complex flow structures. Field observations and measurements suggest that such thunderstorm outflows and their nonlinear coupling with the ambient shear may produce long-lived squall lines.

The interaction of gravity currents with background shear has been the subject of several previous studies. Some of these aim to extend the basic gravity current model of Benjamin (1968) to idealized ambient conditions such as constant shear or discrete velocity jumps (cf. Xu (1992), Liu and Moncrieff (1996)). Just like Benjamin's original model, these extensions usually require an empirical closure assumption for determining the gravity current velocity, which can result in uncertainty regarding the model predictions. On the other hand, Borden and Meiburg (2013) recently introduced an alternative model for gravity currents propagating into quiescent, unstratified ambients that avoids the need for an empirical closure assumption by enforcing the conservation of both horizontal and vertical momentum, based on the vorticity equation. Most recently, Nasr-Azadani and Meiburg (2015) extended this vorticity-based modeling approach to gravity currents propagating into unstratified ambients with constant or two-layer shear and demonstrated very good agreement with DNS results.

Realistic atmospheric gravity current models furthermore need to account for the effects of density stratification, which can result in the formation of internal waves or bores, as well as the thickening or thinning of the gravity current (cf. Rottman and Simpson

(1989), Liu and Moncrieff (1996), White and Helfrich (2012)). Consequently, the present work aims to extend the vorticity-based modeling approach of Borden and Meiburg (2013) to supercritical gravity currents interacting with arbitrary background shear and density stratification, without the need for empirical closure assumptions.

Section 2 defines the problem and presents the model derivation. Section 3 presents the energy and head loss analyses that provide insight into whether or not the model predictions are physically feasible. In section 4 we present comparison between model predictions and DNS simulation results.

2 Model derivation

We consider a gravity current of density ρ_1 and given height h traveling from right to left with unknown constant velocity U_g in a horizontal tank of height H, cf. figure 1a. The tank is filled with ambient fluid that has a known continuous density stratification $\rho_i(y)$ and horizontal velocity $U_i(y)$ far to the left of the current front. To ensure stably-stratified conditions we demand $\rho_i(y) \leq \rho_1$ and $\mathrm{d}\rho_i/\mathrm{d}y \leq 0$.

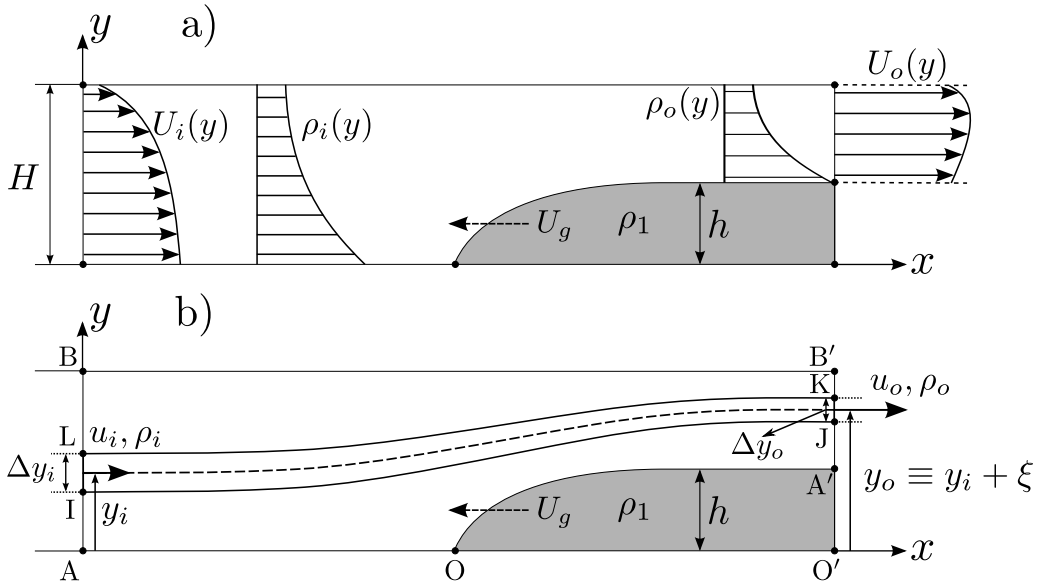

Figure 1: Top: Configuration of a gravity current (shown in gray) propagating into sheared and stably-stratified background fluid. Upstream of the gravity current front, density and horizontal velocity profiles are given as general known functions $\rho_i(y)$ and $U_i(y)$. Bottom: Schematic of the defined control volume IJKL for the problem of a gravity current running into ambient fluid. Conservation of mass and vorticity are derived for this streamtube of width Δy_i, whose center at the inlet is known (y_i) and is displaced at the outlet to an unknown height (y_o). See text for the discussion and derivations.

Without loss of generality, we can rewrite the density function as $\rho_i(y) = \rho_a + \delta\rho_i(y)$, where ρ_a indicates the density at the top wall. In order to obtain a steady flow, we switch to the reference frame moving with the gravity current velocity U_g. In this frame, the upstream velocity reads $u_i(y) = U_i(y) + U_g$.

Let us now consider the narrow streamtube IJKL in figure 1b with the dashed streamline at its center. This streamline of width Δy_i originates from a given height y_i far upstream of the gravity current and is displaced vertically to y_o far downstream of the current front. To describe the unique relationship between these two heights, we introduce

$$y_o = y_i + \xi\,, \tag{1}$$

where the vertical displacement ξ is only a function of the inlet height y_i. For control volume IJKL, the continuity equation takes the form

$$u_i \Delta y_i = u_o \Delta y_o \,. \tag{2}$$

Here, Δy_i and Δy_o denote, respectively, the upstream and downstream width of the streamtube. Next, let us consider the vorticity balance for the streamtube, based on the two-dimensional, steady-state, inviscid vorticity equation in the Boussinesq approximation

$$\mathbf{u} \cdot \boldsymbol{\nabla} \omega = -\hat{g} \frac{\partial \rho^*}{\partial x} \,. \tag{3}$$

Here, $\hat{g}$ $(=g\left(\rho_1 - \rho_a\right)/\rho_a)$ and ρ^* $(=\left(\rho - \rho_a\right)/\left(\rho_1 - \rho_a\right))$ represent the reduced gravity and dimensionless density, respectively. Note that we do not assume the flow to be hydrostatic in the vicinity of the gravity current front and the pressure does not appear in the vorticity balance due to Boussinesq approximation. By applying Gauss' divergence theorem to the streamtube of width Δy_i, equation 3 yields

$$\oint_\Gamma \omega \mathbf{u} \cdot \mathbf{n} \, \mathrm{d}\Gamma = -\iint_A \hat{g} \frac{\partial \rho^*}{\partial x} \, \mathrm{d}A \,. \tag{4}$$

Here, Γ, A and $\mathbf{n}$ denote the boundary, area, and unit outer normal vector of the streamtube of width Δy_i, respectively. We assume that the density field is non-diffusive, so that the density is constant along each streamline. Integrating the vorticity conservation equation 4 for control volume IJKL, applying the mass conservation equation 2, and letting $\Delta y_i \to 0$ we arrive at

$$u_i \omega_i + \hat{g} \frac{(y_o - y_i)}{(\rho_1 - \rho_a)} \frac{\mathrm{d}\rho_i}{\mathrm{d}y_i} = u_i \omega_o \,. \tag{5}$$

Since the flow is assumed to be horizontal far up- and downstream of the gravity current front, the vorticity values in equation 5 take the form $\omega_i = -\mathrm{d}u_i/\mathrm{d}y_i \,, \omega_o = -\mathrm{d}u_o/\mathrm{d}y_o$. To further simplify equation 5, streamline displacement ξ (equation 1) is used to relate the derivative of any variable $(\cdot)$ w.r.t. the outlet height to its derivative w.r.t. the inlet height

$$\frac{\mathrm{d}(\cdot)}{\mathrm{d}y_o} = \frac{\mathrm{d}(\cdot)}{\mathrm{d}y_i} \frac{1}{1 + \xi'} \,. \tag{6}$$

Here, ξ' denotes the derivate of ξ with respect to y_i. In the remainder, a prime indicates the derivative with respect to y_i. In the limit as $\Delta y_i \to 0$, thus, the mass conservation equation 2 gives $u_o(y_o) = u_i(y_i)/\left(1 + \xi'\right)$. We further employ equation 1 to re-write the vorticity conservation equation 5 and arrive at

$$\xi'' u_i^2 + \xi'(1 + \xi')(2 + \xi') u_i u_i' - \xi(1 + \xi')^3 \hat{g} \rho_i' / (\rho_1 - \rho_a) = 0 \,. \tag{7}$$

Equation 7 represents a second order nonlinear ODE for the vertical streamline displacement ξ as a function of the upstream velocity and density profiles. The required two boundary conditions are obtained from geometrical considerations, cf. figure 1

$$\mathrm{AOA}' : \; \xi(y_i = 0) = h \,, \qquad \mathrm{BB}' : \; \xi(y_i = H) = 0 \,. \tag{8}$$

Since, in the reference frame moving with the front, the gravity current velocity U_g enters into the upstream velocity, we require an additional equation to compute U_g. This can be

obtained by integrating the vorticity equation 4 for a thin control volume that includes the vortex sheet separating the gravity current and the ambient fluid (OA′ in figure 1b)

$$\left.\frac{u_o^2}{2}\right|_{y_o=h} = \hat{g}h\frac{\rho_1-\rho_i(y_i=0)}{\rho_1-\rho_a} \rightarrow \xi'(0) = \frac{U_i(0)+U_g}{\sqrt{2\hat{g}h\cdot(\rho_1-\rho_i(0))/(\rho_1-\rho_a)}} - 1\,. \tag{9}$$

Equation 9 provides us with an extra equation to obtain U_g, while solving equation 7 and its two boundary conditions (see equation 8) for $\xi(y_i)$.

3 Energy loss and head loss analysis

For given upstream velocity and density profiles, equation 7 allows us to compute the gravity current velocity U_g as a function of the current height, along with the downstream density and velocity profiles. In order to check if the resulting flow is physically possible, energy and/or head loss analysis can be utilized. Note that, unlike Benjamin (1968) and Xu (1992) who enforce a zero head loss along a specific streamline for closure, our assessment of the flow's energy budget is performed *a posteriori*, and it is not required to solve for the gravity current velocity U_g.

We begin by computing the head loss $\delta_{\mathrm{BB}'}$ along the top wall, cf. figure 1. Here Bernoulli's equation takes the form

$$p_{\mathrm{B}} + \left.\frac{1}{2}\rho_a u_i^2\right|_{y_i=H} = p_{\mathrm{B}'} + \left.\frac{1}{2}\rho_a u_o^2\right|_{y_o=H} + \delta_{\mathrm{BB}'}\,. \tag{10}$$

Evaluating the head loss $\delta_{\mathrm{BB}'}$ requires information on the pressure drop $\Delta p = p_{\mathrm{B}'} - p_{\mathrm{B}}$ along the top wall. This can be obtained from the Boussinesq form of the horizontal momentum equation integrated across the entire channel

$$\int_0^H \left(p_i + \rho_a u_i^2\right)\,\mathrm{d}y = \int_0^H \left(p_o + \rho_a u_o^2\right)\,\mathrm{d}y\,. \tag{11}$$

We assume stress-free conditions at the top and bottom walls and further compute Δp by

$$\begin{aligned} p_{\mathrm{B}'} - p_{\mathrm{B}} = -\frac{1}{H}\Bigg\{ &\frac{1}{2}\left(\rho_1-\rho_a\right)gh^2 + h\int_0^H \delta\rho_i g(1+\xi')\,\mathrm{d}y_i - \rho_a\int_0^H \frac{\xi'}{1+\xi'}u_i^2\,\mathrm{d}y_i \\ &+ \int_0^H (1+\xi')\left(\int_{y_i}^H \delta\rho_i(1+\xi')g\,\mathrm{d}\eta\right)\mathrm{d}y_i - \int_0^H\left(\int_{y_i}^H \delta\rho_i g\,\mathrm{d}\eta\right)\mathrm{d}y_i\Bigg\}\,. \end{aligned} \tag{12}$$

Based on this pressure drop, we can now evaluate the head loss $\delta_{\mathrm{BB}'}$ along the top wall from equation 10. However, we note that for stratified ambients the head loss will vary across the streamlines, so that it is more informative to evaluate the energy loss in the streamwise direction integrated over the entire channel height. Towards that end, we write the energy equation for the entire control volume as

$$\dot{E}_i = \dot{E}_o + \delta\dot{E}\,. \tag{13}$$

Here, $\dot{E}_i$, $\dot{E}_o$ and $\delta\dot{E}$ denote the up- and downstream energy fluxes, as well as the energy loss across the gravity current front. To compute $\delta\dot{E}$, we evaluate the up- and downstream energy integrals

$$\dot{E}_i = \int_0^H u_i\left(p_i + \frac{1}{2}\rho_a u_i^2 + \rho_i g y\right)\mathrm{d}y\,,\quad \dot{E}_o = \int_h^H u_o\left(p_o + \frac{1}{2}\rho_a u_o^2 + \rho_o g y\right)\mathrm{d}y\,, \tag{14}$$

and arrive at

$$\delta\dot{E} = -(p_{\mathrm{B}'} - p_{\mathrm{B}}) \int_0^H u_i \, \mathrm{d}y_i + \int_0^H \delta\rho_i g \xi u_i \, \mathrm{d}y_i + \int_0^H u_i \left(\int_{y_i}^H \xi' \delta\rho_i g \, \mathrm{d}\eta \right) \mathrm{d}y_i$$
$$-\frac{1}{2}\rho_a \int_0^H u_i^3 \left(1 - \frac{1}{(1+\xi')^2} \right) \mathrm{d}y_i \,. \qquad (15)$$

For a detailed derivation of head loss and energy loss analyses, we refer the reader to Nasr-Azadani and Meiburg (2016).

4 Model predictions *vs.* simulation results

For given upstream density and velocity profiles, this section discusses the properties of a gravity current as a function of its height, and it compares model predictions with two-dimensional Direct Numerical Simulation (DNS) results. The present framework allows us to move beyond highly idealized models, and to consider more general nonlinear velocity and density profiles. To illustrate this point, we will in the following focus on ambient velocity and density profiles that decay exponentially across the channel height. As a representative example we choose the profiles

$$\rho_i^*(y_i^*) = 0.8149 e^{-4y_i^*} - 0.0149 \,, \qquad u_i^*(y_i^*) = \left(0.9027 e^{-y_i^*} - 0.5706 \right) + U_g^* \,. \qquad (16)$$

Hereafter, the *-symbol refers to a dimensionless quantity. We employ the channel height H, buoyancy velocity $\sqrt{\hat{g}H}$, and density difference $(\rho_1 - \rho_a)$ as the reference scales and define the dimensionless quantities via $\mathbf{x}^* \equiv \mathbf{x}/H \,, \mathbf{u}^* \equiv \mathbf{u}/\sqrt{\hat{g}H} \,, \rho^* \equiv (\rho - \rho_a)/(\rho_1 - \rho_a) \,, p^* \equiv p/(\rho_a \hat{g} H) \,, t^* \equiv t/(H/\sqrt{\hat{g}H}) \,, \dot{E}^* \equiv \dot{E}/(\rho_a \hat{g}^{3/2} H^{5/2})$. For the given upstream velocity and density profiles (equation 16), we evaluate the displacement function ξ^* and the gravity current velocity U_g^* as functions of the current height.

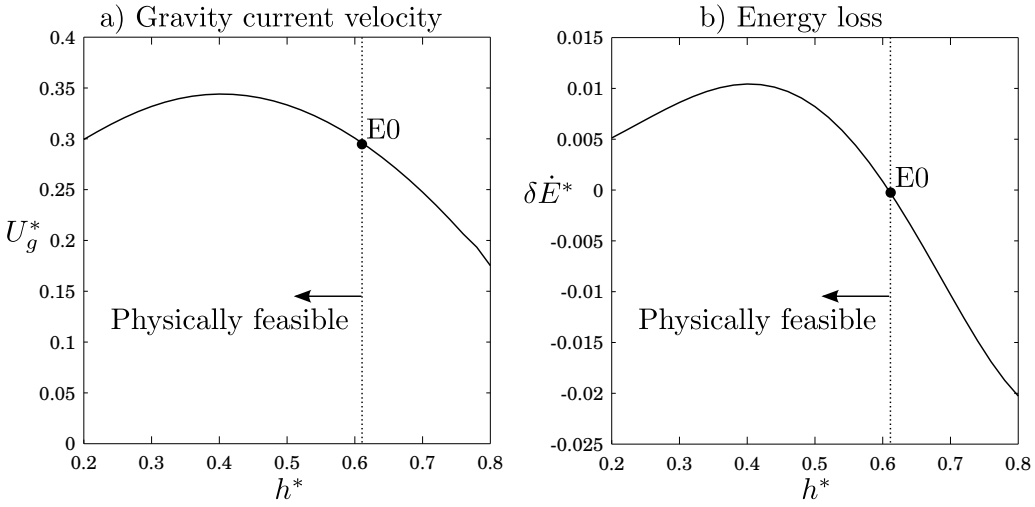

Figure 2: a) Gravity current velocity as a function of the current height. b) Energy loss (equation 15) as a function of the current height. In both a) and b), the inflow density and horizontal velocity profiles are given by equations 16. E0 indicates the zero energy loss case, with a current height $h^* = 0.61$. To the left of the vertical line, the energy loss is positive, so that the solutions are physically meaningful.

Figure 2a depicts the gravity current velocity U_g^* as a function of the current height h^*. We observe a maximum at $h^* \approx 0.4$. The location of this maximum and its value strongly

depend on the ambient shear and stratification. To assess whether or not the obtained solutions are physically feasible, figure 2b shows the corresponding energy loss $\delta\dot{E}^*$ (see equation 15). The zero energy loss case is indicated by the vertical dotted line. To the left of this line, i.e. for $h^* \leq 0.61$, the energy loss is positive, which indicates that the solutions are physically meaningful. For $h^* > 0.61$, on the other hand, negative energy loss values suggest that the corresponding flows cannot be realized without external energy supply.

We now proceed to compare the model predictions against DNS simulation results. Towards this end, we initialize the flow field with a current that has the height corresponding to zero energy loss, as indicated by E0 in figure 2. This case corresponds to $h^* = 0.61$ and $U_g^* = 0.3$. The initial conditions in the DNS simulations are based on the density field and velocity field obtained from model predictions. The simulation is carried out in the reference frame moving with the current velocity predicted by the model. Hence, the agreement between simulation result and model prediction can be assessed by the degree to which the current front remains in place throughout the simulation. We allow the flow to develop in 'time' until a nearly steady state is reached.

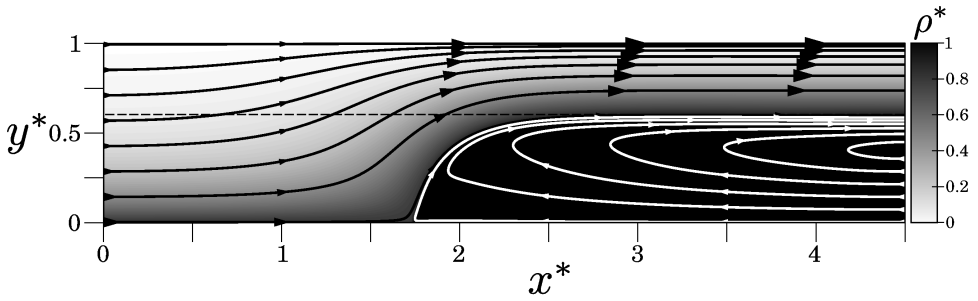

Figure 3: Steady state streamlines along with the density field for a DNS simulation with $Re^* = 2,500$ (see figure 2). The quasisteady current height is close to the value 0.61 predicted by the model (dashed line) for a flow with zero energy loss (case E0).

The simulation is performed by our in-house code TURBINS (Nasr-Azadani and Meiburg (2011)). TURBINS is a finite-difference code which employs TVD-RK3 temporal integration along with a fractional-step projection method to solve the Navier-Stokes equations in the Boussinesq approximation (see Nasr-Azadani and Meiburg (2011) and Nasr-Azadani et al. (2013)).

The computational domain has dimensions $L_x^* \times L_y^* = 4.5 \times 1$, with prescribed inflow and convective outflow boundaries in the horizontal direction. We refer the reader to Nasr-Azadani and Meiburg (2016) for the details of numerical setup.

Figure 3 visualizes the steady-state density field along with the streamlines at time $t^* = 60$. Downstream of the frontal region, the gravity current height approaches the analytical value corresponding to zero energy loss (shown by the dashed line) very closely. After an initial transient period, the flow reaches quasi-steady conditions characterized by a small, approximately constant velocity of $u_f^* = \mathrm{d}x_f^*/\mathrm{d}t^* \approx 0.005$. This indicates that the relative difference between the model prediction for zero energy loss ($U_g^* = 0.3$) and the front velocity recorded in the viscous Navier-Stokes simulation ($U_g^* = 0.3 - u_f^*$) is close to 1.6%, suggesting good agreement between model prediction and simulation result.

Due to existence of viscous effects in the DNS simulation, a weak internal recirculation inside the gravity current body forms, as shown in figure 3. Xu and Moncrieff (1994)

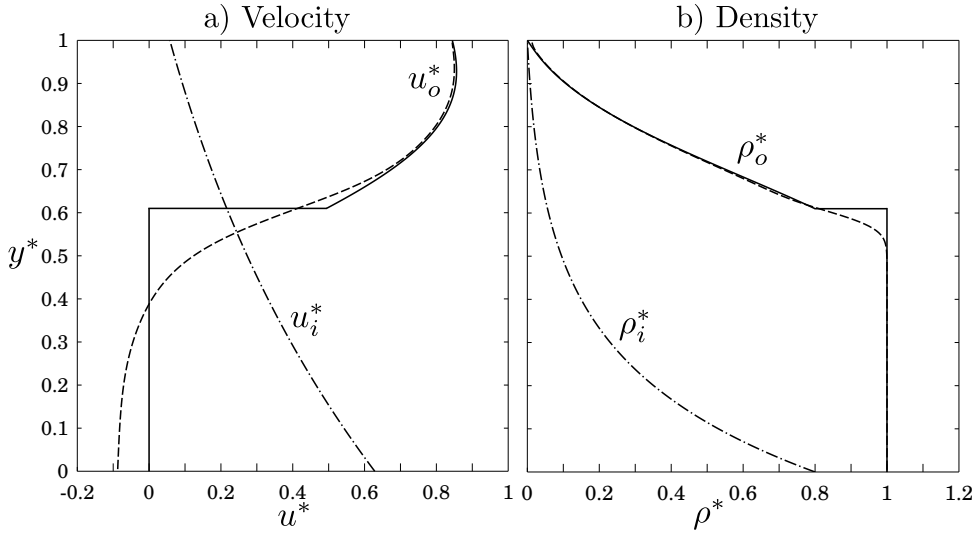

Figure 4: Vertical distribution of a) horizontal velocity and b) density plotted at $x^* = 4$ obtained from simulation E0. Very good agreement is observed between the DNS findings (dashed lines) and theoretical predictions (solid lines). Dashed lines depict the inlet density and velocity profiles.

demonstrate that the influence of the internal circulation on the frontal region and the propagation velocity of the gravity current is small.

Figure 4 compares the quasi-steady density and velocity profiles near the downstream boundary with the model predictions. For completeness, the prescribed inflow velocity and density profiles are shown by dashed-dotted lines. Away from the interface, the simulation results closely duplicate the model predictions. Near the interface, the discontinuities in u^* and ρ^* are smeared out by the presence of diffusion in the simulation. Interestingly, the downstream velocity exhibits a local maximum value at $y_o^* = 0.93$, which

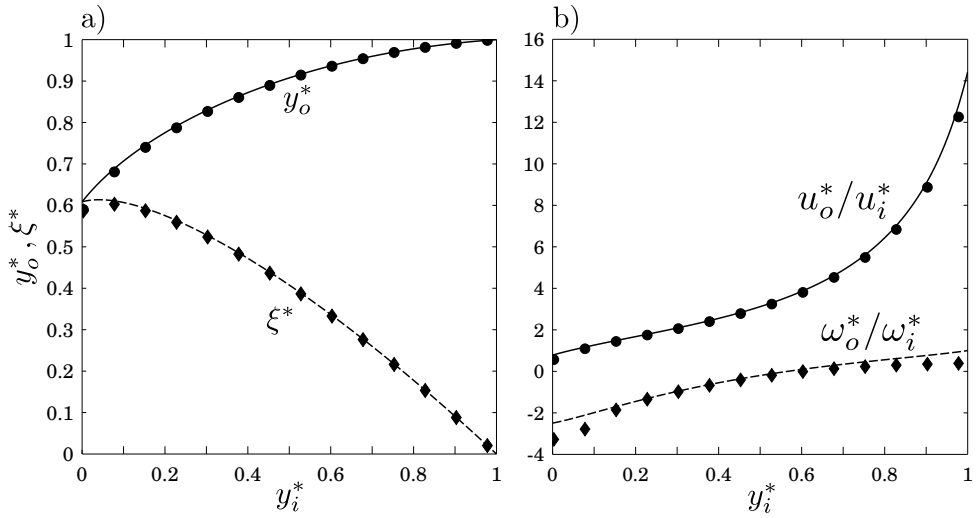

Figure 5: a) Vertical distribution of streamline displacement function ξ^* and outlet streamline location y_o^* computed for case E0. b) Outlet to inlet velocity and vorticity ratio plotted for problem E0. With the presence of background stratification and the resulting baroclinic vorticity, the outlet vorticity changes sign at $\xi^* = 0.36$ ($y_i^* = 0.57$) which causes a maximum in the velocity at the outlet region. RK4 numerical method is employed to solve the ODE in equation 7. Bullets and diamonds are computed from the DNS results.

corresponds to $\xi^* = 0.36$, cf. figure 5a. This height corresponds to the point where the

outflow to inflow vorticity ratio $\omega_o^*/\omega_i^* = 1 - \xi^*\rho^{*'}/\{u^*u^{*'}\}$ reaches a zero value (see the dashed line in figure 5b). This change in the sign of the outflow vorticity ratio, and the corresponding outflow velocity maximum, are achievable only due to the existence of background stratification.The bullets and diamonds shown in figure 5 are from the DNS results. Despite slight differences at the interfacial region which is mainly due to the viscous effects, our theoretical predictions follow the DNS results very closely.

References

Benjamin, T. B. (1968). Gravity currents and related phenomena. *Journal of Fluid Mechanics*, 31(2):209–248.

Borden, Z. and Meiburg, E. (2013). Circulation based models for Boussinesq gravity currents. *Physics of Fluids*, 25(10):101301.

Bryan, G. H. and Rotunno, R. (2014). The optimal state for gravity currents in shear. *Journal of the Atmospheric Sciences*, 71(1):448–468.

Linden, P. (2012). *Gravity current–Theory and laboratory experiments*. Cambridge University Press.

Liu, C. and Moncrieff, M. W. (1996). An analytical study of density currents in sheared, stratified fluids including the effects of latent heating. *Journal of the atmospheric sciences*, 53(22):3303–3312.

Meiburg, E. and Kneller, B. (2010). Turbidity currents and their deposits. *Annual Review of Fluid Mechanics*, 42(1):135–156.

Moncrieff, M. W. (1992). Organized convective systems: Archetypal dynamical models, mass and momentum flux theory, and parametrization. *Quarterly Journal of the Royal Meteorological Society*, 118(507):819–850.

Nasr-Azadani, M. and Meiburg, E. (2015). Gravity currents propagating into shear. *Journal of Fluid Mechanics*, 778:552–585.

Nasr-Azadani, M. M., Hall, B., and Meiburg, E. (2013). Polydisperse turbidity currents propagating over complex topography: Comparison of experimental and depth-resolved simulation results. *Computers & Geosciences*, 53(0):141–153.

Nasr-Azadani, M. M. and Meiburg, E. (2011). TURBINS: An immersed boundary, Navier-Stokes code for the simulation of gravity and turbidity currents interacting with complex topographies. *Computers & Fluids*, 45(1):14–28.

Nasr-Azadani, M. M. and Meiburg, E. (2016). Gravity currents propagating into ambients with arbitrary shear and density stratification: vorticity-based modelling. *Quarterly Journal of the Royal Meteorological Society*, 142(696):1359–1370.

Rottman, J. and Simpson, J. (1989). The formation of internal bores in the atmosphere-a laboratory model. *Royal Meteorological Society, Quarterly Journal*, 115:941–963.

Simpson, J. E. (1997). *Gravity currents: In the environment and the laboratory*. Cambridge University Press, second edition.

White, B. L. and Helfrich, K. R. (2012). A general description of a gravity current front propagating in a two-layer stratified fluid. *Journal of Fluid Mechanics*, 711:545–575.

Xu, Q. (1992). Density currents in shear flows-a two-fluid model. *Journal of the Atmospheric Sciences*, 49(6):511–524.

Xu, Q. and Moncrieff, M. W. (1994). Density current circulations in shear flows. *Journal of the Atmospheric Sciences*, 51(3):434–446.